

Ref.
FAA-02-04

DOT-VNTSC-FAA-02-04

FogEye UV Sensor System Evaluation: Phase I Report

Kevin L. Clark
David C. Burnham
Leo Jacobs

U.S. Department of Transportation
Research and Special Programs Administration
John A. Volpe National Transportation Systems Center
Cambridge, MA 02142-1093

Final Report
September 2002

Prepared for

**U.S. Department of Transportation
Federal Aviation Administration
800 Independence Avenue, SW
Washington, DC 20591**

This document is available to the public
through the National Technical Information
Service, Springfield, VA 22161



U.S. Department of Transportation
Research and Special Programs Administration

Notice

This document is disseminated under the sponsorship of the Department of Transportation in the interest of information exchange. The United States Government assumes no liability for its contents or use thereof.

Notice

The United States Government does not endorse products or manufacturers. Trade or manufacturers' names appear herein solely because they are considered essential to the objective of this report.

REPORT DOCUMENTATION PAGE

Form Approved
OMB No. 0704-0188

Public reporting burden for this collection of information is estimated to average 1 hour per response, including the time for reviewing instructions, searching existing data sources, gathering and maintaining the data needed, and completing and reviewing the collection of information. Send comments regarding this burden estimate or any other aspect of this collection of information, including suggestions for reducing this burden, to Washington Headquarters Services, Directorate for Information Operations and Reports, 1215 Jefferson Davis Highway, Suite 1204, Arlington, VA 22202-4302, and to the Office of Management and Budget, Paperwork Reduction Project (0704-0188), Washington, DC 20503.

1. AGENCY USE ONLY (Leave blank)		2. REPORT DATE September 2002		3. REPORT TYPE AND DATES COVERED Final Report June 2002 – September 2002	
4. TITLE AND SUBTITLE FogEye UV Sensor System Evaluation: Phase I Report				5. FUNDING NUMBERS FA24G/A2534	
6. AUTHOR(S) Kevin L. Clark, David C. Burnham, Leo Jacobs					
7. PERFORMING ORGANIZATION NAME(S) AND ADDRESS(ES) U.S. Department of Transportation Research and Special Programs Administration John A. Volpe National Transportation Systems Center Cambridge, MA 02142-1093				8. PERFORMING ORGANIZATION REPORT NUMBER DOT-VNTSC-FAA-02-04	
9. SPONSORING/MONITORING AGENCY NAME(S) AND ADDRESS(ES) U.S. Department of Transportation Federal Aviation Administration 800 Independence Avenue, SW Washington, DC 20591				10. SPONSORING/MONITORING AGENCY REPORT NUMBER	
11. SUPPLEMENTARY NOTES					
12a. DISTRIBUTION/AVAILABILITY STATEMENT This document is available to the public through the National Technical Information Service, Springfield, Virginia 22161.				12b. DISTRIBUTION CODE	
13. ABSTRACT (Maximum 200 words) FogEye technology uses the solar-blind region of the ultraviolet spectrum to develop sensors or systems that are unaffected by sunlight. The U.S. Congress asked the Federal Aviation Administration (FAA) to investigate the feasibility of applying FogEye technology to aviation-related problems. This report presents results of the FogEye UV Sensor/System Evaluation for Phase I, which compared the measurements of a FogEye transmissometer to those of visible light transmissometers. Several FogEye transmissometer configurations were tested at the Volpe National Transportation Systems Center's (Volpe Center) Otis Weather Test Facility in Bourne, Massachusetts. Test results were favorable—indicating that FogEye equipment can be solar blind, though care must be taken to avoid all responses to other regions of the spectrum. The effective ultraviolet (UV) extinction coefficient measured in fog by the FogEye transmissometer is about half the visible-light extinction coefficient measured by a standard transmissometer. This result was expected, based on the theoretical understanding of light scattering from fog, and is a consequence of the wide fields of view of the FogEye transmitter and receiver. Conclusions thus far are that UV technology has merit and FogEye assessments should continue as planned to determine effective aviation applications.					
14. SUBJECT TERMS FogEye transmissometer, fog hazard, solar blind, ultraviolet extinction coefficient, ultraviolet technology				15. NUMBER OF PAGES 38	
				16. PRICE CODE	
17. SECURITY CLASSIFICATION OF REPORT Unclassified	18. SECURITY CLASSIFICATION OF THIS PAGE Unclassified	19. SECURITY CLASSIFICATION OF ABSTRACT Unclassified	20. LIMITATION OF ABSTRACT		

PREFACE

FogEye technology uses the solar-blind region of the ultraviolet spectrum to develop sensors or systems that are not affected by sunlight. The U.S. Congress asked the Federal Aviation Administration (FAA) to investigate the feasibility of applying FogEye technology to aviation-related problems. The FAA's Office of Surface Technology Assessment (AND-520) has taken responsibility for this investigation and has requested the support of the Volpe National Transportation Systems Center (Volpe Center).

The FogEye equipment tested has been provided by Norris Electro Optical Systems, who have also provided inputs to the discussion section (Appendix B) of this report.

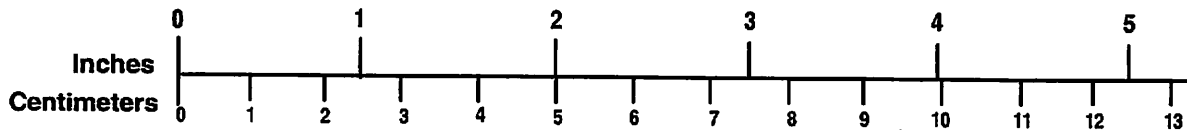
METRIC/ENGLISH CONVERSION FACTORS

ENGLISH TO METRIC

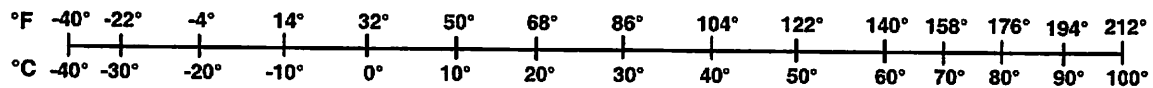
METRIC TO ENGLISH

<p>LENGTH (APPROXIMATE)</p> <p>1 inch (in) = 2.5 centimeters (cm) 1 foot (ft) = 30 centimeters (cm) 1 yard (yd) = 0.9 meter (m) 1 mile (mi) = 1.6 kilometers (km)</p>	<p>LENGTH (APPROXIMATE)</p> <p>1 millimeter (mm) = 0.04 inch (in) 1 centimeter (cm) = 0.4 inch (in) 1 meter (m) = 3.3 feet (ft) 1 meter (m) = 1.1 yards (yd) 1 kilometer (km) = 0.6 mile (mi)</p>
<p>AREA (APPROXIMATE)</p> <p>1 square inch (sq in, in²) = 6.5 square centimeters (cm²) 1 square foot (sq ft, ft²) = 0.09 square meter (m²) 1 square yard (sq yd, yd²) = 0.8 square meter (m²) 1 square mile (sq mi, mi²) = 2.6 square kilometers (km²) 1 acre = 0.4 hectare (ha) = 4,000 square meters (m²)</p>	<p>AREA (APPROXIMATE)</p> <p>1 square centimeter (cm²) = 0.16 square inch (sq in, in²) 1 square meter (m²) = 1.2 square yards (sq yd, yd²) 1 square kilometer (km²) = 0.4 square mile (sq mi, mi²) 10,000 square meters (m²) = 1 hectare (ha) = 2.5 acres</p>
<p>MASS - WEIGHT (APPROXIMATE)</p> <p>1 ounce (oz) = 28 grams (gm) 1 pound (lb) = 0.45 kilogram (kg) 1 short ton = 2,000 pounds (lb) = 0.9 tonne (t)</p>	<p>MASS - WEIGHT (APPROXIMATE)</p> <p>1 gram (gm) = 0.036 ounce (oz) 1 kilogram (kg) = 2.2 pounds (lb) 1 tonne (t) = 1,000 kilograms (kg) = 1.1 short tons</p>
<p>VOLUME (APPROXIMATE)</p> <p>1 teaspoon (tsp) = 5 milliliters (ml) 1 tablespoon (tbsp) = 15 milliliters (ml) 1 fluid ounce (fl oz) = 30 milliliters (ml) 1 cup (c) = 0.24 liter (l) 1 pint (pt) = 0.47 liter (l) 1 quart (qt) = 0.96 liter (l) 1 gallon (gal) = 3.8 liters (l) 1 cubic foot (cu ft, ft³) = 0.03 cubic meter (m³) 1 cubic yard (cu yd, yd³) = 0.76 cubic meter (m³)</p>	<p>VOLUME (APPROXIMATE)</p> <p>1 milliliter (ml) = 0.03 fluid ounce (fl oz) 1 liter (l) = 2.1 pints (pt) 1 liter (l) = 1.06 quarts (qt) 1 liter (l) = 0.26 gallon (gal) 1 cubic meter (m³) = 36 cubic feet (cu ft, ft³) 1 cubic meter (m³) = 1.3 cubic yards (cu yd, yd³)</p>
<p>TEMPERATURE (EXACT)</p> <p>$[(x-32)(5/9)] \text{ } ^\circ\text{F} = y \text{ } ^\circ\text{C}$</p>	<p>TEMPERATURE (EXACT)</p> <p>$[(9/5)y + 32] \text{ } ^\circ\text{C} = x \text{ } ^\circ\text{F}$</p>

QUICK INCH - CENTIMETER LENGTH CONVERSION



QUICK FAHRENHEIT - CELSIUS TEMPERATURE CONVERSION



For more exact and or other conversion factors, see NIST Miscellaneous Publication 286, Units of Weights and Measures. Price \$2.50 SD Catalog No. C13 10286

Updated 8/17/98

TABLE OF CONTENTS

<u>Section</u>	<u>Page</u>
1. INTRODUCTION.....	1
1.1 Background.....	1
1.2 Test Objective and Methodology	1
1.3 Landing System Discussion.....	1
2. TEST CONFIGURATION.....	3
3. EXPECTATIONS	5
4. TEST CHRONOLOGY.....	7
4.1 Receiver R1 – 500-Foot Baseline.....	7
4.2 Receiver R2 – 500-Foot Baseline.....	7
4.3 Receiver 2 – 1,000-Foot Baseline.....	7
5. DATA COLLECTION AND ANALYSIS.....	9
5.1 Data Recording.....	9
5.2 AGC Response	9
5.3 Fog Events	10
6. CONCLUSIONS	17
7. FUTURE TESTING.....	19
A. APPENDIX A – US RVR EQUATIONS.....	A-1
A.1 Reporting Increments	A-1
A.2 Product Calculation	A-1
A.2.1 Koschmieder’s Law	A-1
A.2.2 Allard’s Law.....	A-1
B. APPENDIX B - FOG EYE LANDING SYSTEM PERFORMANCE EXPECTATIONS	B-1
B.1 Analysis.....	B-1
B.2 Discussion.....	B-1

LIST OF FIGURES

<u>Figure</u>		<u>Page</u>
1.	Phase-1 Test Configuration	3
2.	Log Gain vs. Linear AGC Voltage	9
3.	Log Gain vs. Log AGC Voltage.....	9
4.	Strip chart for June 20, 2002.....	11
5.	Strip chart for June 21, 2002.....	12
6.	Strip chart for June 30, 2002.....	13
7.	Extinction Coefficient Scatter Plots with Linear Fits for Three Fog Events (6/20/02 top, 6/21/02 middle, and 6/30/02 bottom) and Two Gain Equations	14
8.	Extinction Coefficient Scatter Plots with Quadratic Fits for Three Fog Events (6/20/02 top, 6/21/02 middle, and 6/30/02 bottom).....	15

LIST OF TABLES

<u>Table</u>		<u>Page</u>
1.	FogEye Ultraviolet Transmissometer, Model No. 07MF4-2040001-2	4
2.	Calculated Diffraction Scattering Angle.....	5
3.	AGC Values	9

EXECUTIVE SUMMARY

High traffic levels related to adverse weather conditions and fog have often been accompanied by rising numbers of aircraft incidents due to low visibility. Such incidents can lead to catastrophic accidents as dramatized by the Air China Flight 162 accident, in which heavy fog and rain shrouding the destination airport was the primary cause of a crash killing 114 people.* Because of ongoing problems associated with reduced visibility operations, emphasis on countermeasures has increased in the United States and Europe. The extreme variability in density, predictability, and location of the fog hazard, however, complicates the task of improving airport safety conditions.

The Federal Aviation Administration (FAA) and the commercial aviation industry seek to develop and evaluate technologies that increase the safety and efficiency of airport operations under low-visibility conditions. The overall goal of these efforts is to provide commercial aircraft with the technology and operating procedures needed for safely achieving the capacity of clear-weather surface operations during adverse-weather conditions. Systems based on visible light, such as runway lights, are degraded by sunlight during the day. FogEye technology operates in the solar-blind ultraviolet region of the spectrum and hence operates as well during the day as at night.

This report presents the results of the FogEye UV Sensor/System Evaluation for Phase I, which compared the measurements of a FogEye transmissometer to those of visible light transmissometers. Phase I provided the first "hands on" FAA experience with FogEye technology and was designed to elucidate the physics of FogEye performance under reduced visibility conditions. Subsequent phases will evaluate more practical applications of FogEye technology, such as trip-wire systems for detecting runway incursions, aircraft detection systems for locating aircraft on a runway or on final approach, and systems to aid aircraft landings during low-visibility conditions.

The Phase I test was conducted at the Volpe National Transportation Systems Center's (Volpe Center) Otis Weather Test Facility at Otis Air National Guard Base in Bourne, Massachusetts. Several FogEye transmissometer configurations were tested and the following results were obtained:

1. FogEye equipment can indeed be solar blind, but care must be taken to avoid all response to other regions of the spectrum.
2. The effective ultraviolet extinction coefficient measured in fog by the FogEye transmissometer is about half the visible-light extinction coefficient measured by a standard transmissometer. This result was expected, based on the theoretical understanding of light scattering from fog, and is a consequence of the wide fields of view of the FogEye transmitter and receiver.

These test results indicate the basic characteristics of ultraviolet (UV) technology are favorable. The conclusions thus far are that the technology has considerable merit and therefore the FogEye assessments should continue as planned, to determine the most attractive and effective aviation applications.

* General Administration of Civil Aviation Administration of China (CAAC), "Air China Crash in Republic of Korea," April 16, 2002.

2. TEST CONFIGURATION

In Phase 1, a FogEye transmissometer consisting of a UV light source and a solar-blind receiver was installed parallel to a conventional visible-light transmissometer (see Figure 1, 1a, and 1b). The direction of transmission was reversed for the FogEye transmissometer to avoid any possible interference between the two transmissometers. The FogEye units had relatively wide beams (approximately 15 degrees, full width) and hence could not detect small angle wide beams. The visible light transmissometers have narrower projector beams and much narrower receiver beams and hence are sensitive to small-angle scattering. In the transmissometer world, the FogEye transmissometer would not be considered an accurate instrument because of its wide beams and hence susceptibility to "forward-scatter" error.

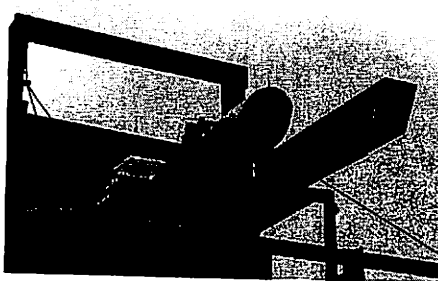
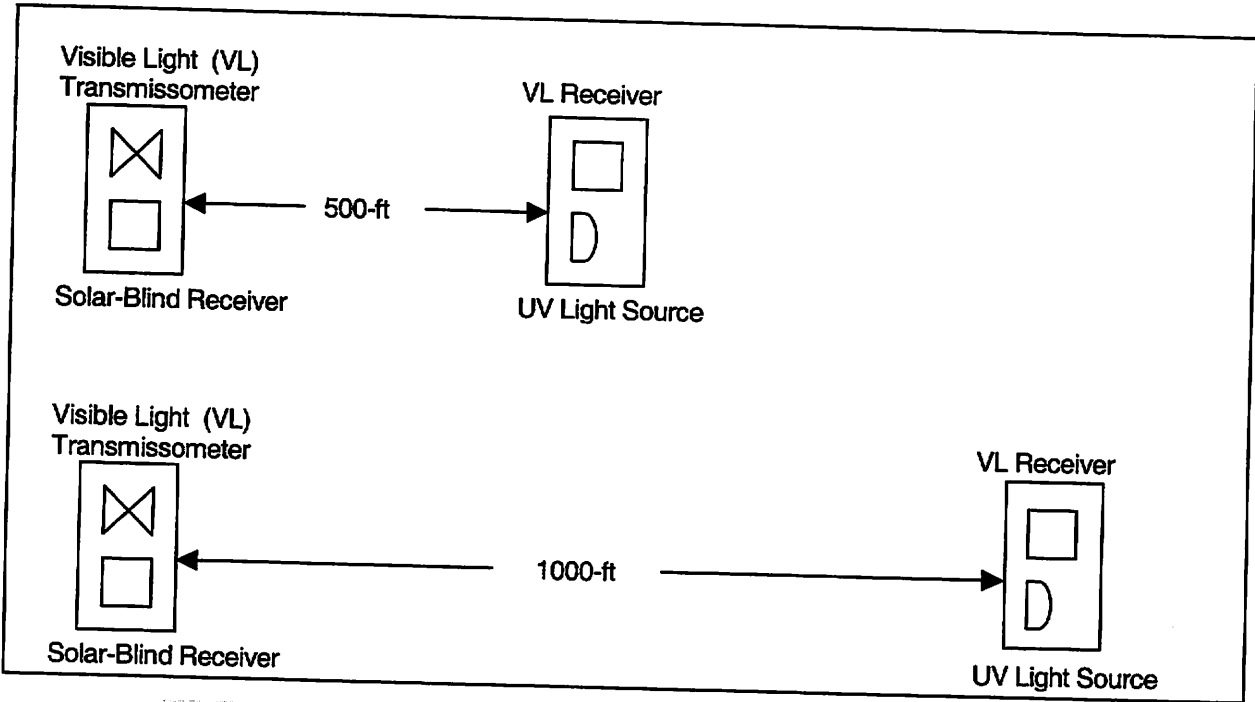


Figure 1a. Solar-Blind Receiver and Visible Light Transmissometer

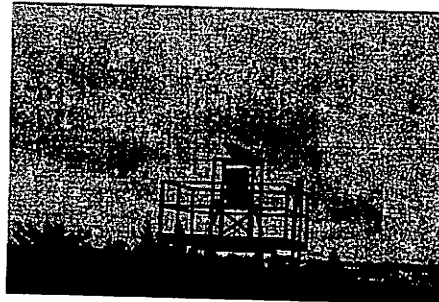


Figure 1b. Visible Light Receiver and Solar-Blind Light Source

Figure 1. Phase-I Test Configuration

Table 1 lists the characteristics of the FogEye transmitter and receiver.

Table 1. FogEye Ultraviolet Transmissometer, Model No. 07MF4-2040001-2

Function	
Measures variations in the atmospheric extinction coefficient at 254 nanometers as atmospheric conditions change from very clear to dense fog, day and night.	
Description	
Consists of a Transmitter and a Receiver, separated by a nominal distance of 1,000 feet.	
Characteristics	
Transmitter	
P/N	07MF4-2046001-1, S/N 1001
Wavelength	254 nanometers
Output Power	42 microwatts/(cm) ² - steradian
Beam Width	12° full width, half power
Excitation Frequency	120 Hertz
Prime Power	115 VAC, 60 Hertz, 20 watts
Receiver	
P/N	07MF4-2047001-1, S/N 1002A
Wavelength	254 nanometers
Sensitivity	3 x 10 ⁸ amps/watt
Field of View	7° full width @ max sensitivity; 15.25° full width, half power
Dynamic Range	3 x 10 ⁵
UV/Visible Signal Attenuation	>10 ⁶
Signal Outputs	
AGC Level	1-3 VDC; Gain Min. to Max.
Detected Signal	5-.01 VDC; Signal Max. to Min. 3 VDC; Nominal Signal
Dynamic Response	
AGC Time Constant	20 seconds
Signal Time Constant	20 seconds
Gain Transfer Curve	Y = -7.3239x ² + 17.418x + 2
Prime Power	115 VAC, 60 Hertz, 1.5 watts
Volpe Weather Test Facility Receiver Configuration Variations	
S/N 1001 (R1) -	500 ft. baseline
AGC:	Not operational
Filter:	Single, No. 1
S/N 1002 (R2) -	500 ft. baseline
AGC:	Operational
Filter:	Single, No. 2
S/N 1002A (R2A) -	1,000 ft. baseline
AGC:	Operational
Filter:	Compound #1

3. EXPECTATIONS

The physics of light scattering from water droplets is well understood; there are two scattering mechanisms that each has a total scattering/absorption cross-section equal to the area of the droplet:

The light directly hitting the droplet is absorbed or scattered in all directions. The absorption is small in the visible and reported to be small also in the solar-blind ultraviolet.

The shadow of the droplet in the incident wave front leads to diffraction scattering in the forward direction. Because this scattered light never enters the droplet, it is not absorbed at all but is totally scattered.

Diffraction scattering from a disk can be calculated[‡] to be:

$$I(\theta) = 4 I_0 (J_1(\beta)/\beta)^2, \quad (1)$$

with $\beta = \pi d \sin \theta / \lambda$ and where

λ = wavelength

d = diameter of disk

I_0 = scattering intensity at zero scattering angle ($\theta = 0$)

J_1 = Bessel function of first order

Equation 1 describes the familiar ring diffraction pattern which has its first zero at $\beta = 3.83$. The central disk contains 84 percent of the total scattered energy. If one integrates Equation 1 to the point where half the diffracted intensity is included, one obtains $\beta_{1/2} = 1.69$. Thus, the half angle for half response becomes:

$$\theta_h = 0.533 \lambda / d \text{ (angle in radians)} \quad (2)$$

Fog droplets are in the range of perhaps 5 to 10 microns. Table 2 shows the calculated half angles for visible light and solar-blind UV light. The calculated FogEye scattering angles are indeed much smaller than the FogEye transmissometer beam sizes. Thus, diffraction scattering will not significantly remove light from the FogEye beams.

Table 2. Calculated Diffraction Scattering Angle

Light	λ (microns)	D (microns)	θ_h (rad)	θ_h (deg)
Visible	0.55	5	0.059	3.4
	0.55	10	0.029	1.7
Solar Blind	0.25	5	0.027	1.5
	0.25	10	0.013	0.8

Note: This theoretical scattering model should be considered in light of limited empirical test data where forward scattering of only 2-3 milliradians was measured at a 2,600 ft range in 700 ft visibility conditions.[§]

[‡] Jenkins, F. A. and White, H. E., Fundamentals of Optics, 3rd ed., 1957, McGraw-Hill, 637 p.

[§] Norris Elector Optical Systems dynamic surface test; September 1996; Greenbrier Valley Airport, West Virginia.

4. TEST CHRONOLOGY

The initial FogEye installation on a 500-foot baseline used a receiver (R1) without automatic gain control (AGC). It was installed from May 17 to May 24, when it was swapped for a new receiver (R2) with AGC.

4.1 Receiver R1 – 500-Foot Baseline

No fog was experienced with R1. Over the period when the data were recorded (May 22 to 24) the sensor extinction coefficient baseline drifted from 0.5 to 3.0 km⁻¹, which corresponds to a transmission variation of about 70 percent to 100 percent. [The actual visible-light extinction coefficient varied by less than 0.2 km⁻¹.] Some of the variation might have been caused by background light (which was not checked by turning off the UV lamp); the apparent extinction coefficient decreased during the daylight hours on some days.

4.2 Receiver R2 – 500-Foot Baseline

A number of fog events were measured by R2 over the period May 25 through 31, but a precise analysis was difficult because of the much greater variation in extinction coefficient baseline (8/km, corresponding to transmission changes from 30 percent to 100 percent). Many of the baseline changes looked like sudden jumps that might be related to drops in power line voltage. The variations were more dramatic during the week than on the weekend. The UV extinction coefficient appeared to be about half the visible-light value, which would be expected because the beams are much wider than the expected narrow forward-scattered half of the UV extinction coefficient.

On May 31, 2002, the first check was made of the background light detected by R2 and was found to be about 2 percent of the intensity of the UV lamp (at 500-foot range). Later measurements at night showed essentially zero background light. Thus, R2 was not solar blind and therefore does not represent the full capability of solar-blind technology.

4.3 Receiver 2 – 1,000-Foot Baseline

On May 31, 2002, some changes were made in the test configuration to improve the evaluation:

1. Provisions were made to turn off the UV lamp for 30 minutes every 2 or 3 hours to measure the background light around the clock.
2. The UV light was moved to the 1,000-foot tower to give a better resolution on the extinction coefficient, given the large variation in baseline signal.
3. Both UV light source and receiver R2 were powered through line-regulating universal power supplies (UPS) in hope of improving their stability. Subsequent measurements typically showed no sudden changes, but some baseline drift was still noted.

The systematic measurements of UV background light through day and night were compared with the ambient light sensor (ALS) that is part of the FAA's New Generation RVR System. The FogEye receiver was pointing approximately south while the ALS was pointing north. The UV background had a well-defined peak at noon, but fell off faster than the visible-light sky brightness toward dawn and dusk.

On May 10, 2002, an additional UV filter was added to Receiver R2 (subsequently termed R2A). Subsequently the background light was zero, even in the middle of the day. The test FogEye system was finally truly solar blind. For R2A the maximum drift in the baseline extinction coefficient was found to be 2 km^{-1} , which is low enough to permit a good comparison of visible and UV extinction coefficients during the fog events.

5. DATA COLLECTION AND ANALYSIS

5.1 Data Recording

The FogEye receivers provided two signals: Signal Voltage and Automatic Gain Control (AGC) Voltage. They were digitized by a Campbell Scientific Model 23X data acquisition module, which sampled at a 10 Hz rate and averaged for 5 seconds. In addition to the 5-second averages, the standard deviations were calculated and recorded. The first sample of the new minute and the 11 prior samples from the prior minute were averaged to generate 1-minute averages that were approximately synchronized with the Otis reference transmissometers.

5.2 AGC Response

Table 3 shows the values provided for the AGC of receiver R2. Figures 2 and 3 plot the values in two forms and fit a quadratic curve to the three points. The equations listed were used to calculate the gain used in the signal analysis.

Table 3. AGC Values

AGC (V)	Gain	
	Value	Exponent
1	1	2
2	3.8	6
3	4.4	8

The curve in Figure 2 was used initially. The operating range of the test was between 1.9 and 2.9 volts where the curve in the fitted line is greatest. Because FogEye personnel used power law gain equations (typically 14th power), the log-log plot in Figure 3 was generated. It gives a straighter line in the operating region and therefore might give a better fit to the actual receiver gain. The power law (i.e., slope) of the fitted line is 17.4 at 1.0 AGC volts and 14.1 at 3.0 AGC volts. Both gain equations will be used in the following analysis.

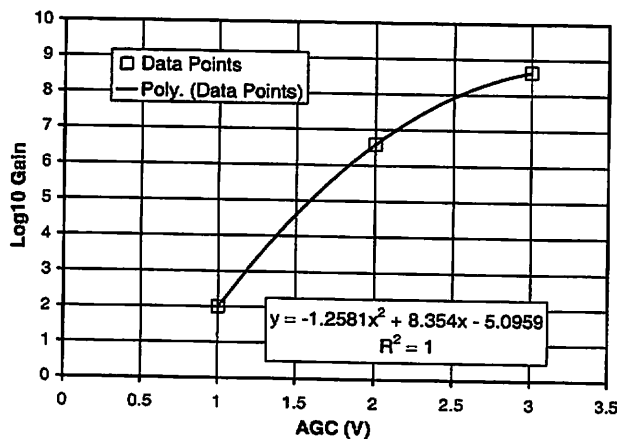


Figure 2. Log Gain vs. Linear AGC Voltage

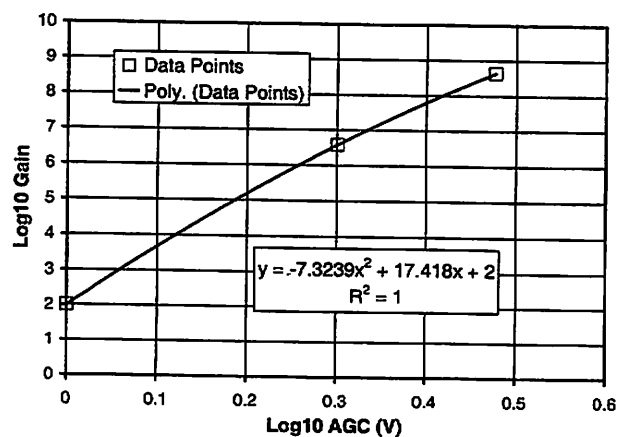


Figure 3. Log Gain vs. Log AGC Voltage

5.3 Fog Events

Figures 4 through 6 show strip charts for the three fog events that will be analyzed. The parameters plotted are:

1. TALS – Ambient light measured by the NG-RVR system
2. S000 – 1,000-foot transmissometer extinction coefficient (includes infrared light)
3. T500 – 500-foot visible light transmissometer extinction coefficient
4. T300 – 300-foot visible light transmissometer extinction coefficient
5. FE2E – FogEye extinction coefficient measurement using 2nd gain equation
6. FE1E – FogEye extinction coefficient using 1st gain equation
7. FE2V – Nominal FogEye voltage using 2nd gain equation
8. FE1V – Nominal FogEye voltage using 1st gain equation
9. FE1S – FogEye Signal voltage
10. FE1A – FogEye AGC voltage

The FogEye light source is turned off for 30 minutes every two hours. When the light is off the signal drops to zero (actually 0.010 volts) and AGC voltage rises to its limiting value of approximately 3 volts (actually 2.975 V). The light source is turned off to verify that the receiver is truly solar blind. Before the second filter was added the signal did not drop to zero during the daytime when the light source was turned off.

The operation of the automatic gain control can be seen in Figures 4 through 6. The signal voltage FE1S is kept near its normal value of 3.0 volts until the AGC voltage (FE1A) reaches its limiting value of about 3.0 volts. Only after the AGC reaches its limit does the signal voltage drop significantly below 3.0 volts.

On June 20, 2002, at approximately 0940 hours the FogEye extinction coefficient reaches the limiting value of 38 km^{-1} , seen when the lamp is turned off. Because the FogEye extinction coefficient is approximately 3 km^{-1} before and after the fog event, the dynamic range of the FogEye transmissometer on the $D = 0.297 \text{ km}$ baseline is approximately $\sigma = 35 \text{ km}^{-1}$, which corresponds to an attenuation of $e^{-\sigma D} = e^{-10.3}$ or about 4.5 decades of dynamic range. This dynamic range is much greater than that achieved for the conventional visible-light transmissometers at Otis, which are limited by the hourly sunlight correction and the minimum transmission of 1/4000.

Figure 7 shows extinction coefficient scatter plots for the three fog events shown in Figures 3-5. The FogEye extinction coefficient is compared to that for T300 using both gain equations. While the gain equation does affect the result slightly, the differences are smaller than the variations in the plots and therefore cannot be used to judge the correctness of the equations.

The scatter plots in Figure 7 include linear least-square-fit lines. The zero offset ranges from 2.5 to 4 km^{-1} and simply represents variation in the 100 percent setting of the FogEye transmissometer. The slopes are more important because they represent the ratio between the FogEye Extinction coefficient and the visible-light extinction coefficient.

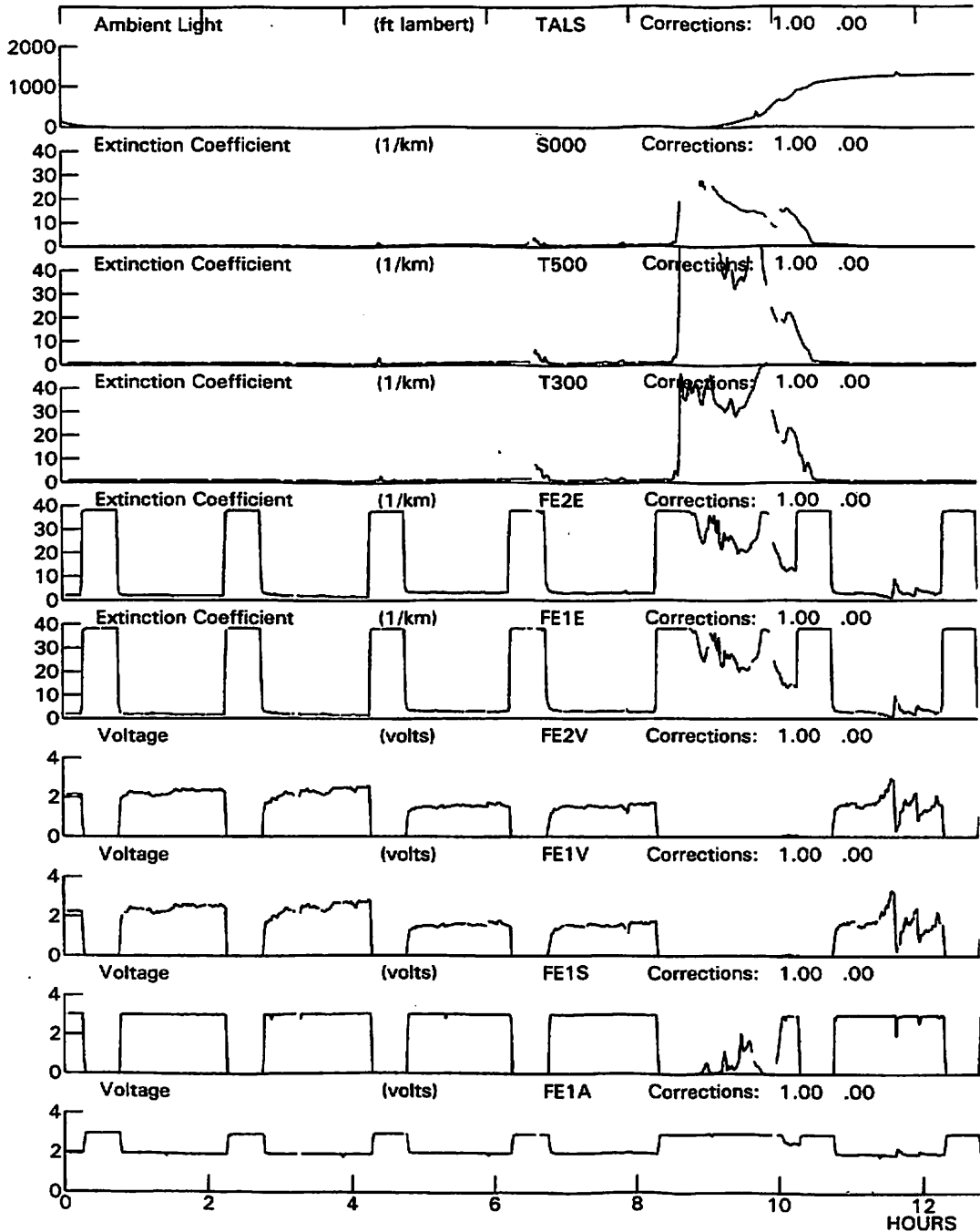


Figure 4. Strip chart for June 20, 2002

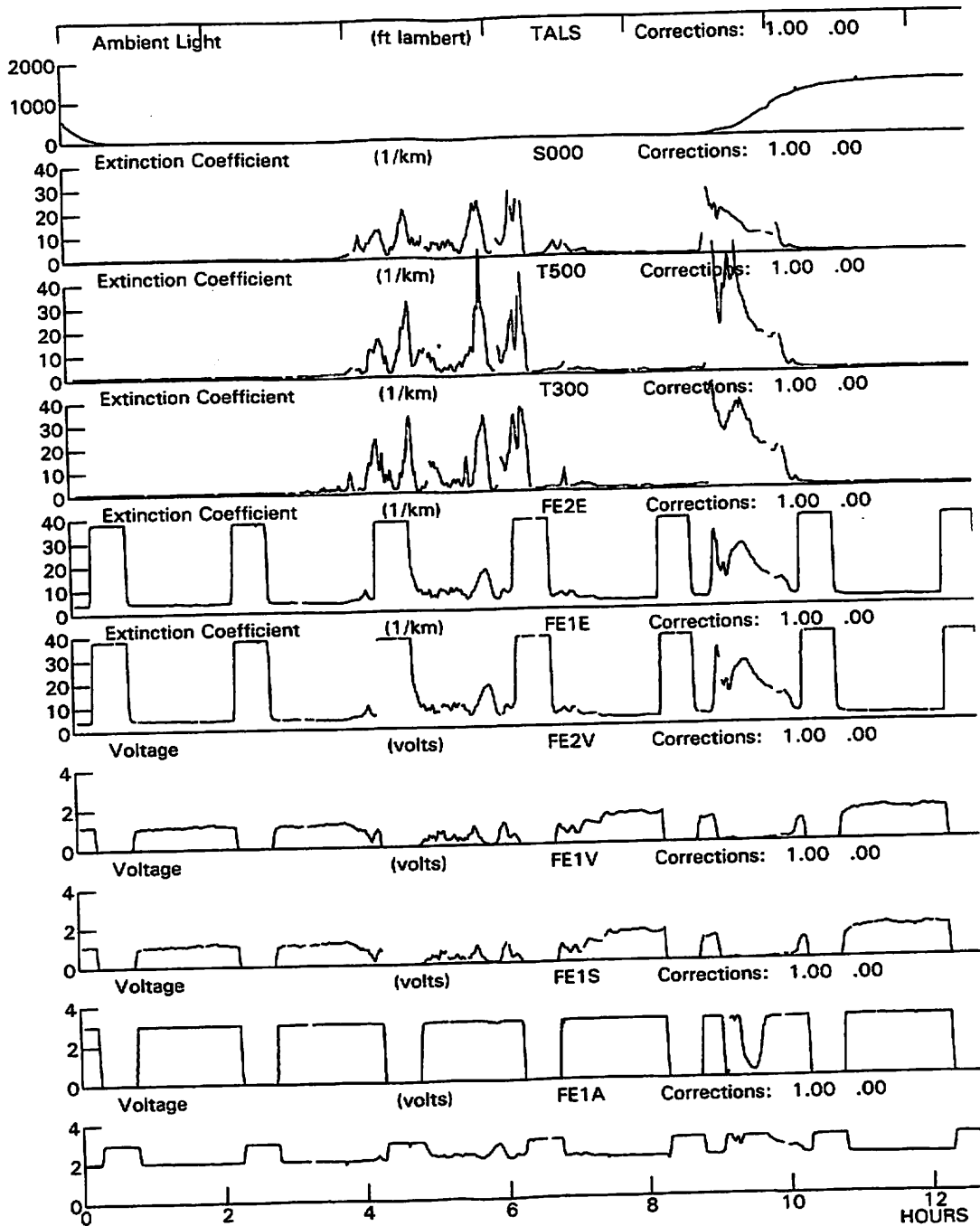


Figure 5. Strip chart for June 21, 2002

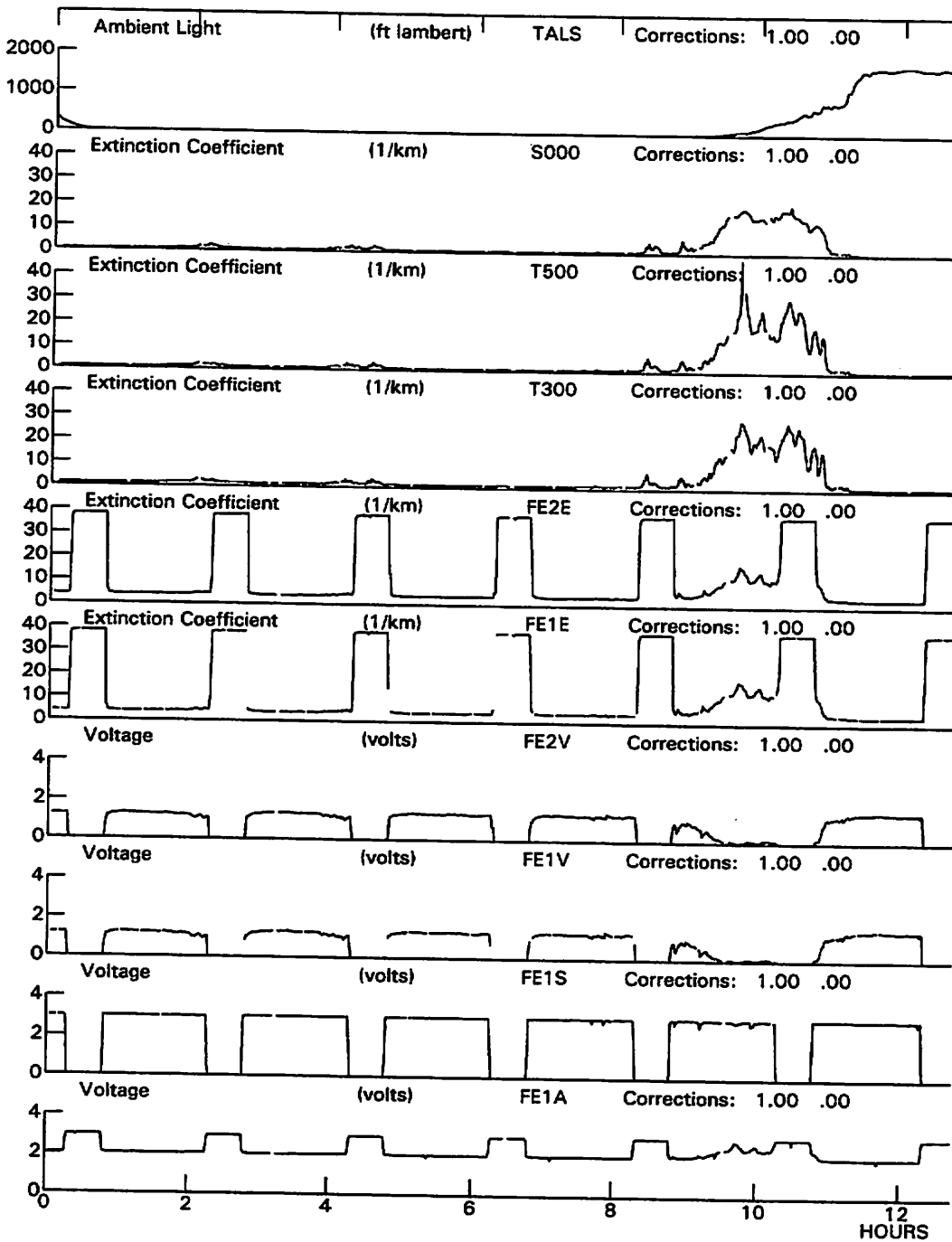


Figure 6. Strip chart for June 30, 2002

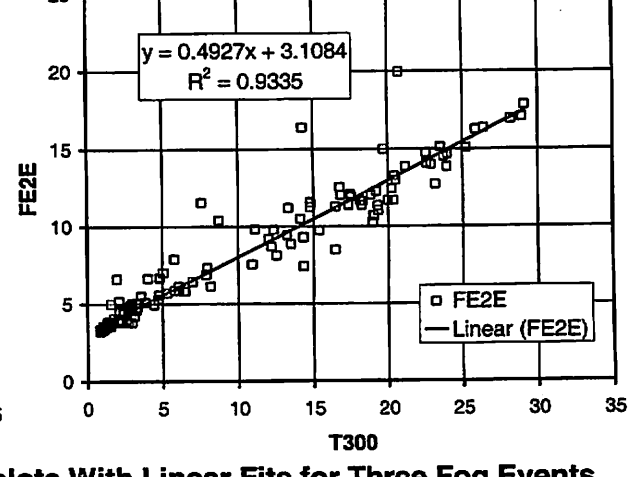
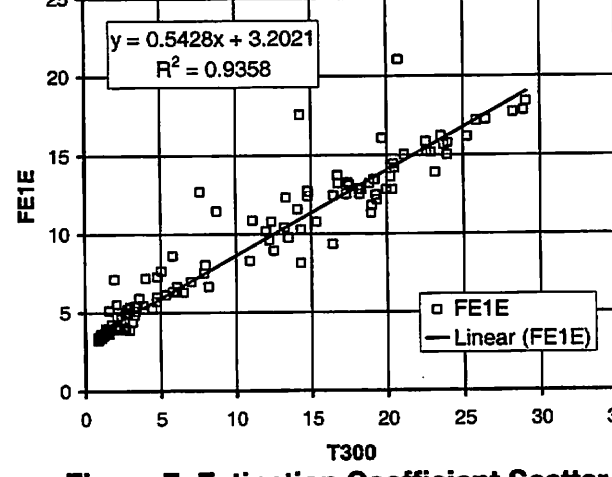
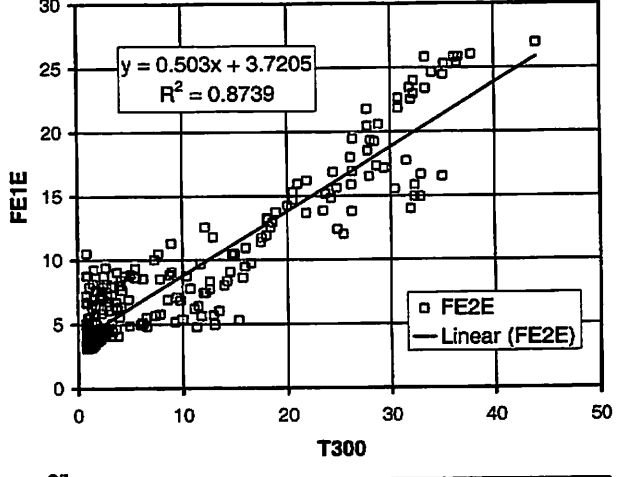
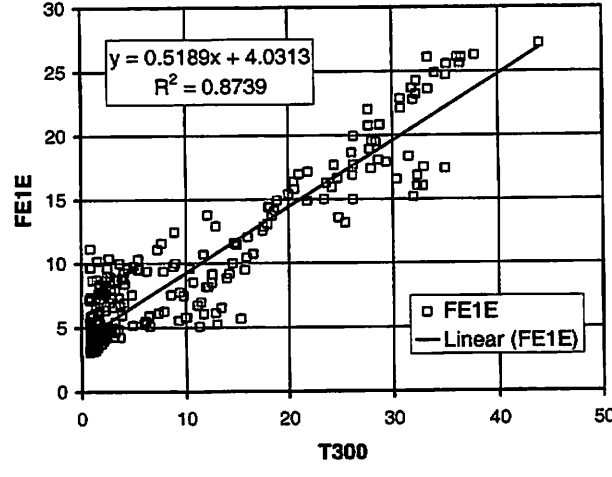
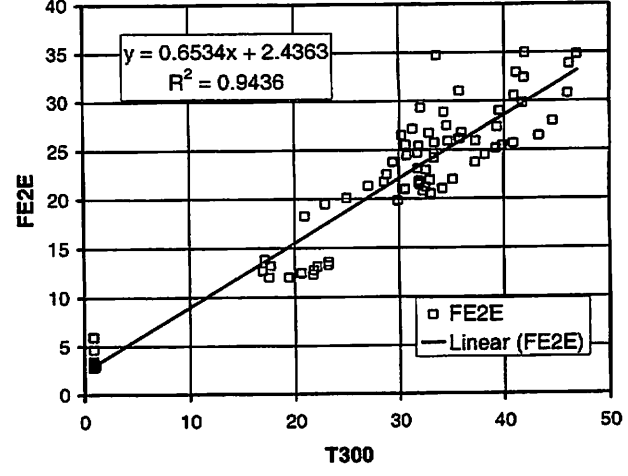
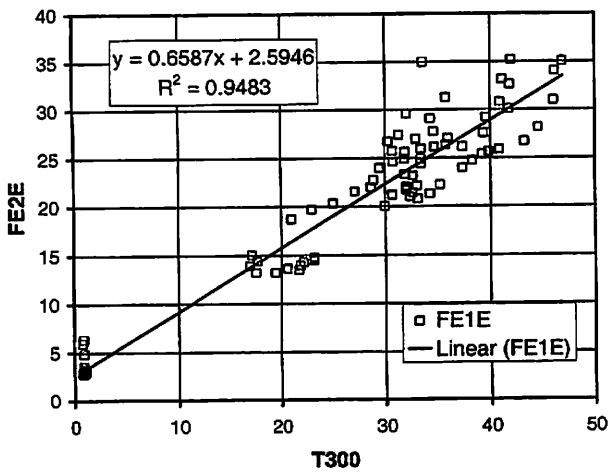


Figure 7. Extinction Coefficient Scatter plots With Linear Fits for Three Fog Events (6/20/02 top, 6/21/02 middle, and 6/30/02 bottom) and Two Gain Equations

The second and third fog events give the expected results that the measured UV extinction coefficient should be about half the visible-light extinction coefficient. The second gain equation gives closer to a slope of exactly half (0.50).

The first event, with a higher slope of 0.65, extends to higher fog density than the other two events and actually reaches the dynamic limit of the FogEye transmissometer (exponential loss of 10.6). It thus represents the equivalent of approximately 10 forward-scatters. With this many scatters, enough light could be lost from the beams to give a larger effective extinction coefficient. The data for the second event (middle plot of Figure 7) also shows values above the fitted line for the highest fog density. The first event also shows more signs of baseline instability (see Figure 4) and the difference in slope might be partly caused by a baseline shift.

Because multiple forward scattering would be difficult to model, Figure 8 presents a simpler approach where a quadratic fit is used to fit the relationship between UV and visible-light extinction coefficients. The extra fit parameter has little impact on the third event with lower extinction coefficients but reduces the linear parameter of the first event closer to the expected value of half (0.56). However, the linear term becomes unrealistically low (0.27) for the second event, presumably because of the systematic scatter in the data points.

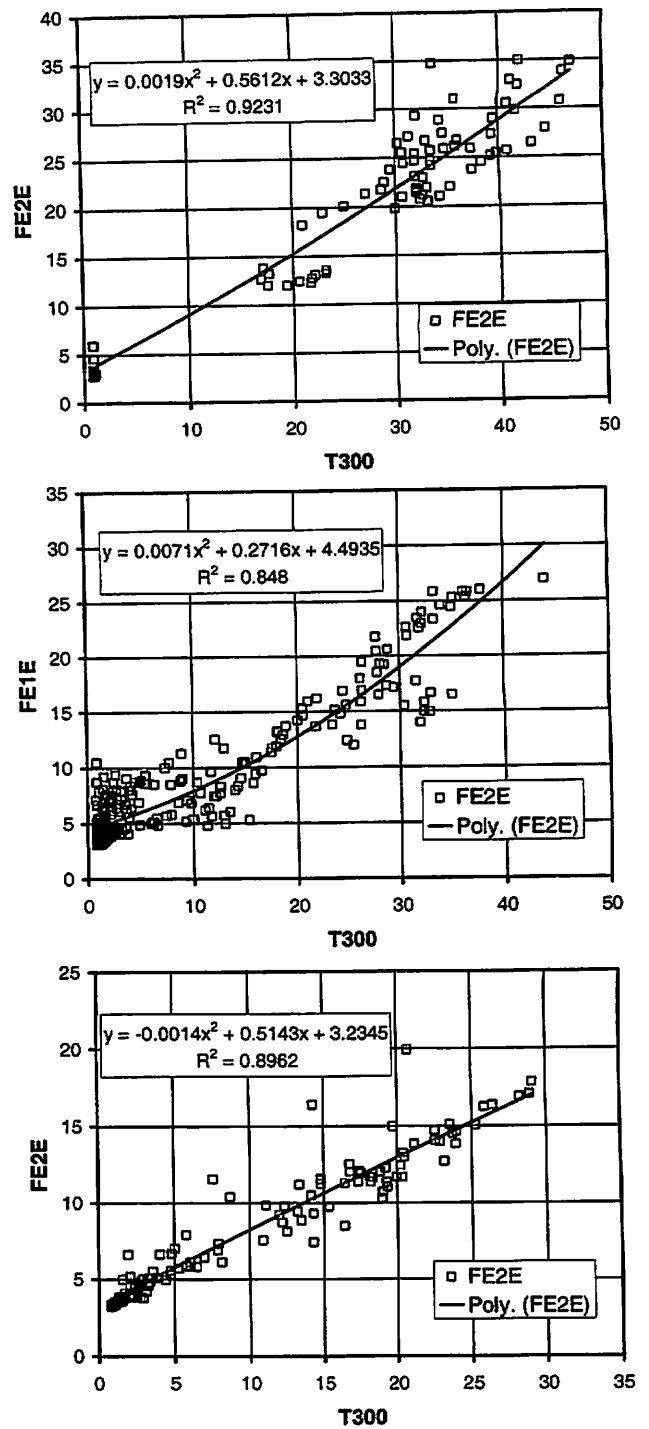


Figure 8. Extinction Coefficient Scatter plots with Quadratic Fits for Three Fog Events (6/20/02 top, 6/21/02 middle, and 6/30/02 bottom)

6. CONCLUSIONS

1. Care must be taken to assure that solar-blind equipment is actually solar blind.
2. Because of its wide beams, in fog, the FogEye transmissometer measures an effective extinction coefficient that is about half the visible-light extinction coefficient. Because this response difference can be explained by the difference in beam widths, this observation is consistent with the assumption that the actual extinction coefficient is the same for visible and solar-blind ultraviolet light. However, the diffraction scattering in the forward direction will be a factor of two narrower for the UV light. The observed elimination of half the fog attenuation for wide FogEye beams might be useful in some application.
3. The FogEye receiver demonstrated a very large dynamic range: approximately 3×10^5 .
4. These test results provide a sound foundation for evaluating practical FogEye applications in subsequent test phases.

7. FUTURE TESTING

The Phase-II FogEye test will evaluate the capabilities of a trip-wire system for detecting runway incursions. Tests will be conducted on a 75-foot baseline (taxiway width) and a 300-foot baseline (maximum runway width). The short baseline test will examine the dynamic response of the trip-wire system. The long baseline test will study the influence of fog on trip-wire dynamic range and especially the possibility that forward-scattered light can bypass the aircraft tire being detected. Two receivers will view one transmitter, one directly and one blocked by a small simulated aircraft tire. Note that the trip-wire system will use one-degree receiver beams to reduce the influence of forward scattered light.

The FogEye Phase-I transmissometer will be reinstalled for Phase II to give additional information about forward scattering. The direct beam will be blocked by a small diameter stop (2 inches) so that the entire signal will come from forward scattered light.

APPENDIX A – US RVR EQUATIONS

A.1 Reporting Increments

The SG-RVR System shall report RVR values in: 100-foot increments from 100 feet through 800 feet; 200-foot increments from 800 through 3,000 feet; and, 500-foot increments from 3,000 through 6,500 feet.

A value of 6,500 feet shall be used to report RVR above 6,249 feet. An RVR value of 100 feet shall indicate runway visual range below 150 feet. The reported RVR shall be rounded off (not rounded down) from the calculated value; therefore, the RVR values from 751 feet to 899 feet would be reported as 800 feet.

A.2 Product Calculation

The validity of the VS and ALS measurements shall be checked. Valid values shall be used to calculate 60-second running averages. The RVR product shall be calculated from 60-second running averages of the readings of the VS and the ALS and the last valid reading of the RLIM. The intensities of the runway edge and centerline lights shall be used, as appropriate for the calculated RVR value. Two RVR values shall be calculated: (1) for seeing objects using Koschmieder's Law (only VS is used); and, (2) for seeing lights using Allard's Law (all three sensors are used).

A.2.1 Koschmieder's Law

Koschmieder's Law states:

$$C_t = e^{-\sigma R}$$

Where:

R = RVR

σ = Atmospheric extinction coefficient

C_t = contrast threshold, which is taken as 0.05

Koschmieder's Law shall give zero RVR whenever the ALS reading is below the night limit of 2 Foot-Lamberts (fL). (6.85 cd/m²).

A.2.2 Allard's Law

In metric units, Allard's Law states:

$$E_t = (I/R^2)e^{-\sigma R}$$

Where:

R = RVR in meters (m)

σ = Atmospheric extinction coefficient in m⁻¹

E_t = Visual threshold in lux

I = Runway light intensity in candelas
 and the visual threshold E_t is given by:

$$\log E_t = -5.7 + 0.64 \log B$$

Where B = background luminance (ambient light) in cd/m^2 . A lower threshold on E_t is set at 6.8×10^{-6} lux, which corresponds to the night limit.

The Standard Runway Light Settings of a HIRL, Table A-1, shall be used.

Table A-1. Standard Runway Light Settings

Light Setting	Nominal Intensity (I) Candelas (cd)	
	Edge Lights	Centerline Lights
Step 0 (Off)	0	0
Step 1	15	7.5
Step 2	120	60
Step 3	500	250
Step 4	2,500	1,250
Step 5	10,000	5,000

The nominal intensity of the centerline lights for the same current is half that of the edge lights. Because the centerline lights are located in the runway pavement and are hence more susceptible to contamination than the edge lights, their intensity is degraded by an additional factor of two in calculating the RVR in the following algorithms. Note that for high RVR values the edge lights are more visible because they are brighter than the centerline lights. For low RVR values the centerline lights are more visible than the edge lights because the pilot is within the main beam of the centerline lights but is in the weaker side lobes of the edge lights.

If both the edge light settings and the centerline light settings have values of 1, 2, 3, 4, or 5, then the value to be used for runway light intensity (I) in Allard's Law for certain values of RVR (in feet) shall be in accordance with Table A-2, Runway Light Intensity When Edge and Centerline Settings Match. Note that the centerline light intensity and edge light intensity are taken from the light setting/candela table for the appropriate values of centerline light setting and edge light setting respectively.

Table A-2. Runway Light Intensity When Edge and Centerline Settings Match

No.	Condition	Action
1	RVR < 600	I = 50% of Centerline Light Intensity
2	600 ≤ RVR ≤ 1,000	Interpolate linearly for "I" between a value of 50% of Centerline Light Intensity at 600 feet and 100% of Edge Light Intensity at 1,000 feet
3	RVR > 1,000	I = 100% of Edge Light Intensity

If the edge light setting has a value of 1, 2, 3, 4, or 5 and the centerline light setting has a value of 0 then the value to be used for runway light intensity (I) in Allard's Law for certain values of RVR (in feet) shall be in accordance with Table A-3, Runway Light Intensity When Centerline Setting is 0. Note that if the edge light setting is 0, then, regardless of the centerline light setting, a value of 0 shall be assigned to the Allard's Law solution.

Table A-3. Runway Light Intensity When Centerline Setting is Zero (0)

No.	Condition	Action
1	RVR < 1,000	assign a value of 0 to the Allard's Law solution
2	RVR > 1,000	I = 100% of Edge Light Intensity

APPENDIX B - FOG EYE LANDING SYSTEM PERFORMANCE EXPECTATIONS

The observations with the FogEye transmissometer are consistent with the assumption that the true UV and visible-light extinction coefficients are equal. Under certain assumptions, the expected performance enhancement of a FogEye runway lighting system can then be evaluated using the standard Runway Visual Range (RVR) equations (see Appendix A).

B.1 Analysis

Figure B-1 shows the relationship between the RVR value from Allard's Law (viewing high intensity runway lights at setting 5) and the RVR value from Koschmieder's Law (termed meteorological optical range or MOR) (viewing black objects with contrast threshold of 0.05). Three curves are shown for three values of background luminance (2 = night, 2,000 = day, and 10,000 = bright day). The breaks in the curves are caused by the change from viewing runway edge lights (RVR > 1,000 feet) and runway centerline lights (RVR < 600 feet). Note that Allard's Law RVR for the highest light setting (5) is greater than MOR for most of the operationally significant RVR range (2400 feet and below).

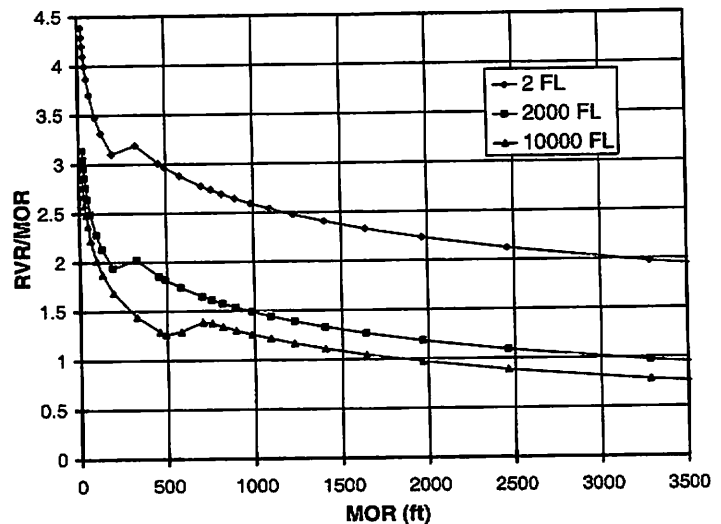


Figure B-1. Allard's Law RVR (Light Setting 5)

The difference between the night (2 FL) and daytime curves (2,000, 10,000 FL) in Figure 9 shows the influence of daylight on viewing runway lights. **If one assumes that the night performance of the runway lights at maximum intensity is comparable to the night and day performance of a solar-blind UV lighting system**, then the differences in the night *and* day curves in Figure 9 can be used to calculate the expected daytime improvement of a UV lighting system and solar-blind UV camera compared to the current high intensity lighting system with human viewing. Figure 10 shows the expected ratio of FogEye (always night) RVR to current RVR for the two daylight brightness values shown in Figure 9. The plots are presented against MOR (top) and daytime RVR (bottom). For example, if the daytime RVR is 1,000 feet (bottom plot Figure 10), the FogEye RVR will be higher by a ratio of 1.7 (1,700 feet) for a brightness of 2,000 FL and a ratio of 2.25 (2,250 feet) for a brightness of 10,000 FL.

Discussion

How comparable are the night RVR values for high intensity runway lights and UV runway lights? The RVR equations assume that brighter lights will always give a higher value of RVR. This assumption fails in two ways:

The light that is scattered out of the beam does not disappear but contributes to the background light. The highest light settings lead to strong attenuation (e.g., $(0.05)^3$ or 4 decades for MOR = 500 feet, RVR = 1500 feet for the 2 FL curve in Figure 9) so that most (99.99 percent in the example) of the scattered light contributes to background. At some level of attenuation the remaining signal will be lost in the background. This effect is multiplied for multiple lights which must be seen individually but all of which contribute to the background. This effect is most notable operationally for approach lights where many lights are located close together. [Note that a UV enhanced landing system must include the approach lights which are the first objects seen at the decision height.]

The large attenuation factors that determine the most distant light visible mean that closer lights will be relatively very bright and may interfere with seeing the farther lights. Sometimes pilots will request a reduction from light setting 5 to light setting 4 to reduce such glare.

A UV camera might suffer from both of these human visual limitations that limit the amount of attenuation that lights can undergo while remaining visible. Thus, because it seems that the visual lighting system is near the practical limits of light attenuation (if not, then brighter runway lights would be installed), it is plausible to assume similar performance for a UV lighting system, as was assumed in generating Figure B-2.

This above comparison assumes that the FogEye Camera system is the same as the human eye. However, there are a number of extra capabilities with respect to the human eye that will enhance its relative performance:

1. The UV background illumination, including the forward and diffusely scattered light, is very much less than the nominal 2 FL used in the computation of the night-time visual RVR.
2. The FogEye Camera has a much larger receiving aperture than the human eye, and operates at the photon noise limit so the limiting brightness is much fainter than the human eye.

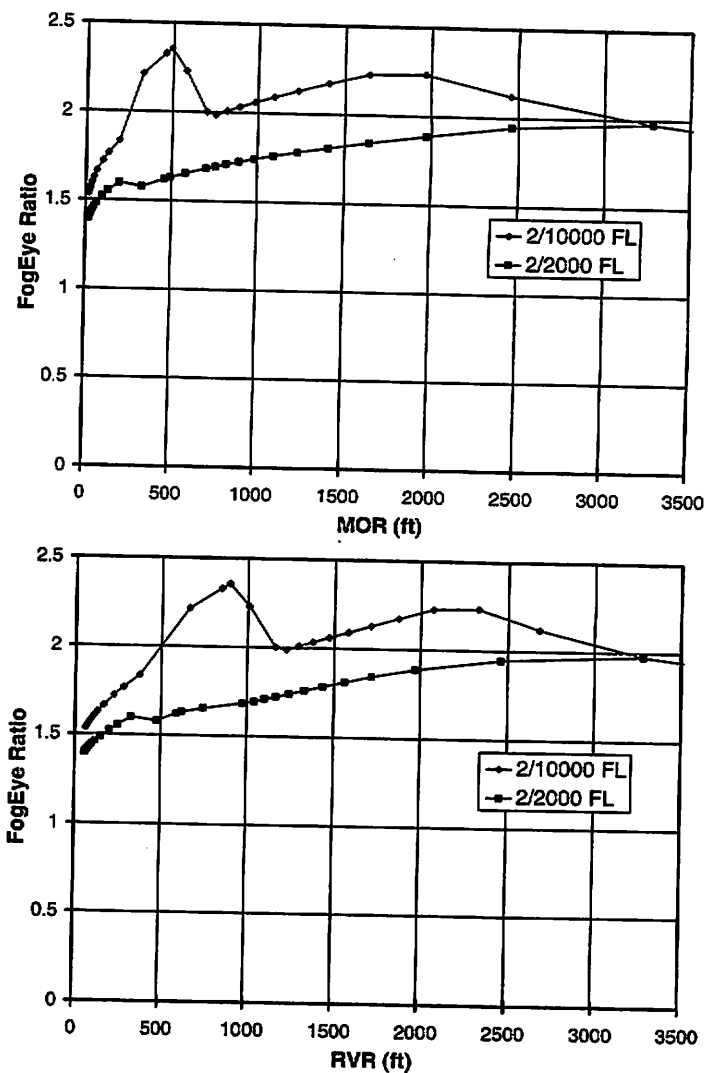


Figure B-2. Expected RVR Improvement for FogEye Compared to Current High Intensity Runway Lighting System

3. The response is linear and might permit better detection of point sources against background light
4. Hardware and Software procedures can block the effect of nearby bright lights.

Further discussion and eventually tests will be needed to resolve the validity of the analysis presented in Figure B-2.